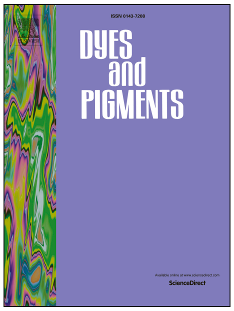

A *t*-butyl modification approach of acceptor moiety for stable deep blue emission in thermally activated delayed fluorescent devices

Yu Jin Kang, Jun Yeob Lee

PII: S0143-7208(16)30925-1
DOI: 10.1016/j.dyepig.2016.11.036
Reference: DYPI 5605

To appear in: *Dyes and Pigments*

Received Date: 9 October 2016
Revised Date: 18 November 2016
Accepted Date: 20 November 2016

Please cite this article as: Kang YJ, Lee JY, A *t*-butyl modification approach of acceptor moiety for stable deep blue emission in thermally activated delayed fluorescent devices, *Dyes and Pigments* (2016), doi: 10.1016/j.dyepig.2016.11.036.

A t-butyl modification approach of acceptor moiety for stable deep blue emission in thermally activated delayed fluorescent devices

Yu Jin Kang, Jun Yeob Lee*

School of Chemical Engineering, Sungkyunkwan University
2066, Seobu-ro, Jangan-gu, Suwon-si, Gyeonggi-do, 440-746, Korea

Fax: (+) 82-31-299-4716
E-mail: leej17@skku.edu
* To whom correspondence should be addressed

Abstract

A t-butyl modification method of an acceptor moiety was developed as a molecular design approach of blue emitters to shift the emission color to deep blue region and to stabilize the emission color according to doping concentration. A phenyl unit of triphenyltriazine acceptor moiety of blue thermally activated delayed fluorescent emitter was modified with either one or two t-butyl units to study the effect of the t-butyl unit on the electroluminescence emission of the blue thermally activated delayed fluorescent emitters. It was found that two t-butyl units introduced in the phenyl unit of the triphenyltriazine shifted the emission color to deep blue emission while keeping the deep blue color over wide doping concentration range.

Key words : deep blue, thermally activated delayed fluorescent emitter, color stability, t-butyl

Introduction

For the last several years, there have been tremendous efforts to explore thermally activated delayed fluorescent (TADF) emitters as high efficiency emitters because of strong need for high efficiency blue emitters overcoming the low theoretical quantum efficiency (QE) of conventional blue fluorescent emitters[1-9]. Currently, the maximum QE of the blue TADF emitters is as high as 25 % by molecular design utilizing all generated excitons by electrical injection for radiative transition process.

Although several classes of blue TADF emitters have been reported, triphenyltriazine type TADF emitters are promising as the blue TADF emitters when both QE and lifetime of the TADF devices are considered. In fact, one of the best lifetime and QE data of the blue TADF devices were realized using tiphenyltriazine acceptor based TADF emitters. The lifetime of the stable blue TADF device was about 50 h up to 80% of initial luminance at 500 cd/m^2 using 9,9',9'',9'''-((6-phenyl-1,3,5-triazine-2,4-diyl)bis(benzene-5,3,1-triyl))tetrakis(9H-carbazole) emitter[10], while the QE of the blue TADF device was 25% using 9,9',9''-(5-(4,6-diphenyl-1,3,5-triazin-2-yl)benzene-1,2,3-triyl)tris(9H-carbazole) emitter[11].

It is true that a great progress of the lifetime and QE of the triazine type blue TADF devices was made by rational molecular design utilizing all excitons for light-emission process, but the TADF devices still suffer from red shift of emission color according to the increase of TADF doping concentration by strong intermolecular interaction originated by donor-acceptor type chemical structure[13-17]. In particular, planar structure of the diphenyltriazine acceptor facilitated intermolecular interaction of the triazine based TADF emitters, which shifted the emission wavelength of the TADF devices to long wavelength[12]. Until now, electron transport type bis[2-(diphenylphosphino)phenyl]ether oxide (DPEPO) is the most popular host material for blue TADF devices and the device performances were optimized at a relatively high doping concentration above 10%. Therefore, the emission color of the blue TADF devices was red-shifted compared to the original photoluminescence (PL) emission, which made it difficult to develop deep blue TADF devices.

In this work, a molecular design blocking an acceptor moiety with a t-butyl substituent was proposed as a method of suppressing red-shift of emission color according to doping concentration of TADF emitters. The number of t-butyl units in the molecular structure was controlled, which demonstrated that the increase of t-butyl units could stabilize the emission spectrum of TADF devices according to TADF doping concentration and shift the emission spectrum to short wavelength.

Results and discussion

The t-butyl modification of the diphenyltriazine acceptor unit was the color stabilizing design approach because intermolecular interaction would be suppressed by the t-butyl blocking group. The t-butyl unit was used to modify the acceptor unit because t-butyl modification of donor unit would strengthen the donor character and lead to red shift of emission color[13]. Donor moiety of the TADF emitters in this work was carbazole and only the acceptor moiety was substituted with t-butyl modified phenyl unit.

Preparation method of two t-butyl modified TADF emitters, 9,9'-(5-(4,6-bis(4-(tert-butyl)phenyl)-1,3,5-triazin-2-yl)-1,3-phenylene)bis(9H-carbazole) (tDCzTrz) and 9,9'-(5-(4,6-bis(3,5-di-tert-butylphenyl)-1,3,5-triazin-2-yl)-1,3-phenylene)bis(9H-carbazole) (DtDCzTrz), is explained in **Scheme 1.** The t-butyl modification method of the diphenyltriazine acceptor unit was Grignard reaction of mono- or di- butylated bromobenzene with 2,4,6-trichlorotriazine. Two butylated phenyl units were reacted with 2,4,6-trichlorotriazine by the Grignard reaction, which produced tDCzTrz with mono- t-butylated phenyl unit and DtDCzTrz with di- t-butylated phenyl unit. Work-up and purification procedures of the two TADF emitters were similar.

The effect of the t-butyl modification on the electronic orbital distribution of the TADF emitters was investigated although it may not change the electronic state of the compounds. Molecular orbital distribution were determined using B3LYP/6-31G* basis set of Gaussian 09 program. The ground state simulation results of the TADF emitters in **Figure 1** suggested that the t-butyl modification of the diphenyltriazine acceptor had little effect on the electronic orbital represented by highest occupied molecular orbital (HOMO) and lowest unoccupied molecular orbital (LUMO). As the diphenyltriazine is a strong acceptor, the weakly electron donating t-butyl unit did not alter the HOMO and LUMO irrespective of the number of t-butyl units. The carbazole based donor moieties and diphenyltriazine based acceptor moiety were the HOMO and LUMO determining parts of the TADF emitters. t-butyl modification effect on the HOMO and LUMO values was examined by indirectly measuring the ionization potential (IP) and electron affinity (EA) of the TADF emitters by electrochemically driven cyclic voltammetry (CV). Oxidative voltage scan and reductive voltage scan in **Figure 2** allowed the determination of the IP and EA of the compounds using Ferrocene as the standard material. The IP of the two compounds was not different as inferred from the electronic orbital dispersion. As the t-butyl modification was applied to the acceptor moiety, the IP was not changed in the TADF emitters. The t-butyl modification only changed the EA of the TADF emitters by weak electron donating character of the t-butyl unit. The EA of DtDCzTrz with two t-butyl units became shallow by the electron donating effect of the t-butyl unit. This indicates that the t-butyl substitution of the diphenyltriazine acceptor can control the EA of the TADF emitters. The IP-EA gap of the TADF emitters was widened in the DtDCzTrz emitter as can be confirmed in **Table 1**.

The ultraviolet-visible (UV-vis) absorption, room temperature fluorescent emission and low temperature phosphorescent emission of the two TADF emitters were described in **Figure 3**. The UV-vis absorption spectra of the TADF emitters had nothing to do with the t-butyl substituent because main chromophore of the tDCzTrz and DtDCzTrz was the same. There was slight red-shift of the UV-vis absorption edge in the DtDCzTrz emitter. Considering that the IP-EA gap widening effect of the t-butyl modification, the t-butyl modification affected the PL behaviour of the TADF emitters. Comparing tDCzTrz and DtDCzTrz, the addition t-butyl unit of DtDCzTrz slightly shifted the emission wavelength to short wavelength by the weakened electron acceptor character of the diphenyltriazine acceptor. The fluorescent peak wavelengths of tDCzTrz and DtDCzTrz emitters were 423 nm with a shoulder at 450 nm and 425 nm, respectively. However, the phosphorescent peak appeared at a similar wavelength because the t-butyl modifier had little effect on the degree of conjugation of the TADF compounds. Peak wavelengths of the phosphorescence were 449 nm and 450 nm in the tDCzTrz and DtDCzTrz, respectively. The singlet and triplet energy of the TADF materials were estimated from the onset point of fluorescent and phosphorescent emission peaks and the extra t-butyl unit in the DtDCzTrz slightly increased the singlet-triplet energy splitting. Therefore, the role of the extra t-butyl unit in the synthesized TADF emitters can be summarized as blue shift of emission spectrum and slight increase of singlet-triplet energy splitting.

PL behaviour of the TADF compounds was further studied by analysing PL decay at different temperatures. PL measurement results of tDCzTrz and DtDCzTrz at 10, 100, 200 and 300 k are displayed in **Figure 4**. From the similar PL decay data irrespective of temperature, it can be noticed that the t-butyl modification had little influence on the radiative decay of the TADF emitters. At 10 k and 100 k, the delayed PL component was very weak and the temperature did not alter the delayed PL behaviour of tDCzTrz and DtDCzTrz. However, the weak delayed fluorescence was intensified at 200 k and 300 k by increased TADF emission. Intense delayed emission and quick PL decay were apparent in the PL data, which were generally observed in other TADF emitters.

Two TADF emitters were independently evaluated in the device structure designed for high QE using DPEPO high triplet energy host material. Doping concentration of each emitter was a variable to monitor the change of the emission spectrum. Basic device performances of the blue TADF devices were plotted in **Figure 5**. In all TADF devices, gradual increase of current density and luminance at the same driving voltage was observed by increased doping of the TADF emitters due to hole injection and transport function of the TADF emitters in the poor hole conducting DPEPO host. Although the TADF emitter itself is a hole trapping dopant in the DPEPO host, heavily doped TADF emitters played a role of hole transport medium by hole hopping effect.

External quantum efficiency (EQE) of each TADF device was presented according to emitter doping content in **Figure 6**. Optimum doping concentration of the TADF emitters for high EQE was different in the tDCzTrz and DtDCzTrz devices, and it was 10% in the tDCzTrz and 20% in the DtDCzTrz devices. Increase of the optimum doping concentration by the additional t-butyl unit was observed in the TADF devices. This result can be interpreted by intermolecular interaction blocking role of the t-butyl unit. When DPEPO was the host material, there are two major effects caused by the change of doping concentration, which are concentration quenching and charge balance[16]. High doping concentration is favoured for charge balance due to more hole density, but low doping concentration is preferred for less concentration quenching. If the concentration quenching effect is dominant, optimum doping concentration would be decreased, and vice versa. In the case of the DtDCzTrz, charge balancing effect is more dominant than concentration quenching effect by the additional t-butyl unit, which optimized the EQE at 20%.

The t-butyl unit also exhibited emission spectra stabilizing and blue-shifting function in the doped TADF devices. The electroluminescence (EL) spectra of tDCzTrz and DtDCzTrz devices at 10, 20, 30 and 50% doping concentrations in **Figure 7** apparently testified blue shift of EL emission at the same doping concentration and less red shift of EL emission at high doping concentration by the extra t-butyl unit of DtDCzTrz. The color coordinates of the tDCzTrz devices at 10% and 50% doping concentrations were (0.15, 0.12) and (0.16, 0.19), while those of the DtDCzTrz devices were (0.15, 0.09) and (0.15, 0.13) at the same doping concentrations. Compared with the EL spectra change of the DCzTrz, there was much less change of the EL sepctra according to doping concentration[10]. Moreover, the EL spectra were not affected by driving voltage. Deep blue emission color could be demonstrated by the t-butyl modification approach which suppressed intermolecular interaction between emitters and weakened electron accepting character of the acceptor moiety. Moreover, the suppression of intermolecular interaction between DPEPO and DtDCzTrz may assist the deep blue emission of DtDCzTrz. All device performances of the tDCzTrz and DtDCzTrz devices are shown in Table 2.

Experimental

General information

1,3,5-Tribromobenzene, potassium acetate and 9H-carbazole were purchased from Aldrich Chem. 9H-carbazole was used after purification by recrystallization. 1-Bromo-4-(tert-butyl)benzene, 1-bromo-3,5-di-tert-butylbenzene, and cyanuric chloride purchased from Alfa Aesar Co. were used without purification. Tetrakis(triphenylphosphine)palladium(0) and 1,1´-bis(diphenylphosphino)ferrocene were received from P&H Tech Co. Potassium carbonate, magnesium sulfate, anhydrous 1,4-dioxane, sodium hydride and n-hexane were products of Duksan Sci. Co. These chemicals were used as received. Tetrahydrofuran and toluene was distilled over sodium and calcium hydride. General chemical analysis was reported our previous paper[13-15].

Synthesis

9,9'-(5-(4,4,5,5-tetramethyl-1,3,2-dioxaborolan-2-yl)-1,3-phenylene)bis(9H-carbazole)

The intermediate material was synthesized according to previous literature[10].

2,4-bis(4-(tert-butyl)phenyl)-6-chloro-1,3,5-triazine (1) A solution of 1-bromo-4-(tert-butyl)benzene (4.0 g, 18.7 mmol) in anhydrous THF (10 ml) was added dropwise to a suspension of iodine-activated magnesium (2.3 g, 93.8 mmol) in anhydrous THF (5 ml). After that the reaction mixture was refluxed for 3 h and then cooled to room temperature. The resulting Grignard solution was slowly added to a solution of cyanuric chloride (2.3 g, 12.4 mmol) in anhydrous toluene (50 ml) at room temperature. The mixture was refluxed overnight and was cooled down to room temperature. The reaction mixture was quenched with distilled water and extracted by methylene chloride. The crude product was purified by column chromatography on silica gel using a n-hexane/methylene chloride eluent and a white powder was obtained (2.5 g, yield 62 %).

2-Chloro-4,6-bis(3,5-di-tert-butylphenyl)-1,3,5-triazine (2) A solution of 1-bromo-3,5-di-tert-butylbenzene (5.0 g, 18.5 mmol) in anhydrous THF (15 ml) was added dropwise to a suspension of iodine-activated magnesium (2.2 g, 92.8 mmol) in anhydrous THF (10 ml). After that the reaction mixture was refluxed for 3 h and then cooled to room temperature. The resulting Grignard solution was slowly added to a solution of cyanuric chloride (1.0 g, 5.4 mmol) in anhydrous Toluene (30 ml) at room temperature. The mixture was refluxed for overnight. Work-up procedure of 2 was the same as that of 1 and the product was obtained as a white powder (1.3 g, yield 53 %).

9,9'-(5-(4,6-Bis(4-(tert-butyl)phenyl)-1,3,5-triazin-2-yl)-1,3-phenylene)bis(9H-carbazole) (tDCzTrz) 2,4-Bis(4-(tert-butyl)phenyl)-6-chloro-1,3,5-triazine (1) (0.8 g, 2.1 mmol) and 9,9'-(5-(4,4,5,5-tetramethyl-1,3,2-dioxaborolan-2-yl)-1,3-phenylene)bis(9H-carbazole) (1.3 g, 2.3 mmol) were dissolved in anhydrous THF (30 ml). After 30 min, tetrakis(triphenylphosphine)palladium (15.0 mg, 0.1 mmol) and 2M aqueous potassium carbonate (6.9 g, with distilled water 15 ml) was added in above mixture continuously. The residue was extracted by methylene chloride and distilled water. And then solvent was removed from the resulting mixture under reduced pressure. The crude product was purified by column chromatography on silica gel using n-hexane/methylene chloride. The product was sublimed and obtained as a greenish yellow powder (1.2 g, yield 76 %). ^{1}H NMR (500 MH$_Z$, CDCl$_3$): 9.10 (s, 2H), 8.65-8.63 (d, 4H, J = 5.0 Hz), 8.21-8.19 (d, 4H, J = 3.7 Hz), 8.04-8.03 (t, 1H, J = 1.3 Hz), 7.64-7.62 (d, 4H, J = 4.0 Hz), 7.55-7.53 (d, 4H, J = 4.2 Hz), 7.50-7.46 (t, 4H, J = 5.5 Hz), 7.36-7.35 (t, 4H, J = 2.5 Hz), 1.36 (s, 18H) MS (APCI) *miz* 752.9 [(M)$^+$]. Elemental Analysis calculated for $C_{53}H_{45}N_5$: C, 84.65; H, 6.03; N, 9.31. Found : C, 84.64; H, 6.24; N, 8.75;

9,9'-(5-(4,6-bis(3,5-di-tert-butylphenyl)-1,3,5-triazin-2-yl)-1,3-phenylene)bis(9H-carbazole) (DtDCzTrz) 2-chloro-4,6-bis(3,5-di-tert-butylphenyl)-1,3,5-triazine (2) (1.0 g, 2.0 mmol) and 9,9'-(5-(4,4,5,5-tetramethyl-1,3,2-dioxaborolan-2-yl)-1,3-phenylene)bis(9H-carbazole) (1.2 g, 2.2 mmol) were dissolved in anhydrous THF (30 ml). After 30 min, tetrakis(triphenylphosphine)palladium (15.0 mg, 0.1 mmol) and 2M aqueous potassium carbonate (6.9 g, with distilled water 15 ml) was added in above mixture continuously. Work-up procedure of DtDCzTrz was the same as that of tDCzTrz and the product was obtained as a yellowish green powder after sublimation (1.1 g, yield 63 %). ^{1}H NMR (500 MH$_Z$, CDCl$_3$): 9.0 (s, 2H), 8.65-8.65 (d, 4H, J = 0.7 Hz), 8.20-8.18 (d, 4H, J = 4.0 Hz), 8.12-8.11 (t, 1H, J = 1.3 Hz), 7.76-7.75 (d, 4H, J = 4.0 Hz), 7.70-7.69 (t, 2H, J = 1.1 Hz), 7.50-7.46 (t, 4H, J = 5.5 Hz), 7.36-7.33 (t, 4H, J = 5.1 Hz), 1.41 (s, 36H) MS (APCI) *miz* 865.1 [(M)$^+$]. Elemental Analysis calculated for $C_{61}H_{61}N_5$: C, 84.78; H, 7.11; N, 8.10. Found : C, 84.75; H, 6.98; N, 7.87;

Device Fabrication

All devices reported in this work were fabricated using a thermal evaporator with a vacuum pressure of 1.0 × 10^{-6} torr. To investigate the electroluminescence (EL) performance of the two compounds, we fabricated devices with the optimized structures of indium tin oxide(ITO)/ poly(3,4-ethylenedioxythiophene):poly(styrenesulfonate) (PEDOT:PSS, 60 nm)/ 4,4′-cyclohexylidenebis[N,N - bis(4-methylphenyl) aniline] (TAPC, 20 nm)/ 1,3-bis(N-carbazolyl)benzene (mCP, 10 nm)/ DPEPO:tDCzTrz, or DPEPO:DtDCzTrz (25 nm)/ diphenylphosphine oxide-4-(triphenylsilyl)phenyl (TSPO1, 5 nm)/ 1,3,5-tris(N-phenylbenzimidazole-2-yl)benzene (TPBi, 30 nm)/ LiF (1.5 nm)/ Al (200 nm). Doping concentrations of tDCzTrz and DtDCzTrz in the DPEPO host were 10%, 20%, 30% and 50%, respectively.

Conclusions

In conclusion, a study on the effect of t-butyl modification of an acceptor of TADF emitters on the light emission of blue emitters demonstrated blue-shifting and spectrum stabilizing function of the t-butyl unit. DtDCzTrz TADF emitter with two t-butyl units included phenyl unit showed a deep blue color coordinate of (0.15,0.11) by the blue-shifting effect of the t-butyl unit. Therefore, the t-butyl modification approach of the acceptor would be effective to develop deep blue TADF emitters. .

References

1. Zhang Q, Li J, Shizu K, Huang S, Hirata S, Miyazaki H, Adachi C. Design of Efficient Thermally Activated Delayed Fluorescence Materials for Pure Blue Organic Light Emitting Diodes J. Am. Chem. Soc. 2012;134:14706-14709.

2. Lee CW, Lee JY. Above 30% External Quantum Efficiency in Blue Phosphorescent Organic Light-Emitting Diodes Using Pyrido[2,3-b]indole Derivatives as Host Materials Adv. Mater. 2013;25:5450-5455.

3. Zhang Q, Li B, Huang S, Nomura H, Tanaka H, Adachi C. Efficient blue organic light-emitting diodes employing thermally activated delayed fluorescence Nat. Photon. 2014;8:326-332.

4. Sun JW, Lee JH, Moon CK, Kim KH, Shi HS, Kim JJ. A Fluorescent Organic Light-Emitting Diode with 30% External Quantum Efficiency Adv. Mater. 2014;26:5684-5688.

5. Sun JW, Baek JY, Kim KH, Moon CK, Lee HJ, Kwon SK, Kim YH, Kim JJ. Thermally Activated Delayed Fluorescence from Azasiline Based Intramolecular Charge-Transfer Emitter (DTPDDA) and a Highly Efficient Blue Light Emitting Diode Chem. Mater. 2015;27: 6675-6681.

6. Hirata S, Sakai Y, Masui K, Tanaka H, Lee SY, Nomura H, Nakamura N, Yasumatsu M, Nakanotani H, Zhang Q, Shizu K, Miyazaki H, Adachi C. Highly efficient blue electroluminescence based on thermally activated delayed fluorescence Nat. Mater. 2015;14:330-336.

7. Yook KS, Lee JY. Organic Materials for Deep Blue Phosphorescent Organic Light-Emitting Diodes Adv. Mater. 2012;24:3169-3190.

8. Komatsu R, Sasabe H, Seino Y, Nakao K, Kido J. Light-blue thermally activated delayed fluorescent emitters realizing a high external quantum efficiency of 25% and unprecedented low drive voltages in OLEDs J. Mater. Chem. C. 2016;4:2274-2278.

9. Zhang Q, Tsang D, Kuwabara H, Hatae Y, Li B, Takahashi T, Lee SY, Yasuda T, Adachi C. Nearly 100% internal quantum efficiency in undoped electroluminescent devices employing pure organic emitters Adv. Mater. 2015;27:2096-2100.

10. Kim MG, Jeon SK, Hwang SH, Lee JY. Stable Blue Thermally Activated Delayed Fluorescent

Organic Light-Emitting Diodes with Three Times Longer Lifetime than Phosphorescent Organic Light-Emitting Diodes Adv. Mater. 2015;27:2515-2520.

11. Lee DR, Kim MG, Jeon SK, Hwang SH, Lee CW, Lee JY. Design Strategy for 25% External Quantum Efficiency in Green and Blue Thermally Activated Delayed Fluorescent Devices Adv. Mater. 2015;27:5861-5867.

12. Schmidbauer S, Hohenleutner A, Konig B. Chemical Degradation in Organic Light-Emitting Devices:Mechanisms and Implications for the Design of New Materials Adv. Mater. 2013;25:2114-2129.

13. Cho YJ, Yook KS, Lee JY. High Efficiency in a Solution-Processed Thermally Activated Delayed-Fluorescence Device Using a Delayed-Fluorescence Emitting Material with Improved Solubility Adv. Mater. 2014;26:6642-6646.

14. Kim MG and Lee JY. Engineering the Substitution Position of Diphenylphosphine Oxide at Carbazole for Thermal Stability and High External Quantum Efficiency Above 30% in Blue Phosphorescent Organic Light-Emitting Diodes Adv. Funct. Mater. 2014;24:4164-4169.

15. Cho YJ, Lee JY. A Universal Host Material for High External Quantum Efficiency Close to 25% and Long Lifetime in Green Fluorescent and Phosphorescent OLEDs Adv. Mater. 2014;26:4050-4055.

16. Yoo SG, Jeon SK, Hwang SH, Lee JY. A Strong Hole Transport Type Host Material for High Quantum Efficiency Blue Phosphorescent Organic Light-Emitting Diodes J. Ind. Eng. Chem. 2015;32:72-76.

List of tables

Table 1. Measured photophysical properties of tDCzTrz and DtDCzTrz.

	IP (eV)	EA (eV)	Singlet energy (eV)	Triplet energy (eV)	ΔE_{ST} (eV)	excited state lifetime (μs)
tDCzTrz	-6.17	-3.40	3.14	2.95	0.19	13.9
DtDCzTrz	-6.17	-3.35	3.18	3.01	0.17	12.9

Table 2. Summarized of device performance of tDCzTrz and DtDCzTrz devices at different doping concentrations.

	Doping Concentration (%)	**Maximum Quantum efficiency (%)**	**Maximum Current efficiency (cd/A)**	**Color Coordinate**
tDCzTrz	10	14.5	13.8	0.15,0.12
	20	10.7	12.8	0.15,0.14
	50	5.0	8.9	0.16,0.19
	100	2.6	6.8	0.20,0.24
DtDCzTrz	10	8.8	6.7	0.15,0.09
	20	14.7	14.1	0.15,0.11
	50	6.8	7.7	0.15,0.13
	100	2.0	3.5	0.16,0.14

List of figures

Scheme 1. Synthetic scheme of tDCzTrz and DtDCzTrz,

Figure 1. HOMO and LUMO distribution of tDCzTrz and DtDCzTrz calculated using Gaussian 09 program.

Figure 2. Electrochemical oxidation and reduction curves of tDCzTrz and DtDCzTrz.

Figure 3. UV-Vis and fluorescence and phosphorescence spectra of the tDCzTrz and DtDCzTrz. (Fluorescence spectra are prompt emission of solid film at room temperature and phosphorescence spectra are delayed emission spectra at 77 K.)

Figure 4. Transient PL decay curves of the 10 wt % tDCzTrz (a) and 20 % DtDCzTrz (b) doped DPEPO films.

Figure 5. Current density-voltage-luminance curves of tDCzTrz (a) and DtDCzTrz (b) devices according to doping concentration of dopant materials.

Figure 6. Quantum efficiency–luminance curves of tDCzTrz and DtDCzTrz devices at optimized doping concentration.

Figure 7. Electroluminescence spectra of tDCzTrz (a) and DtDCzTrz (b) devices according to doping concentration of dopant materials.

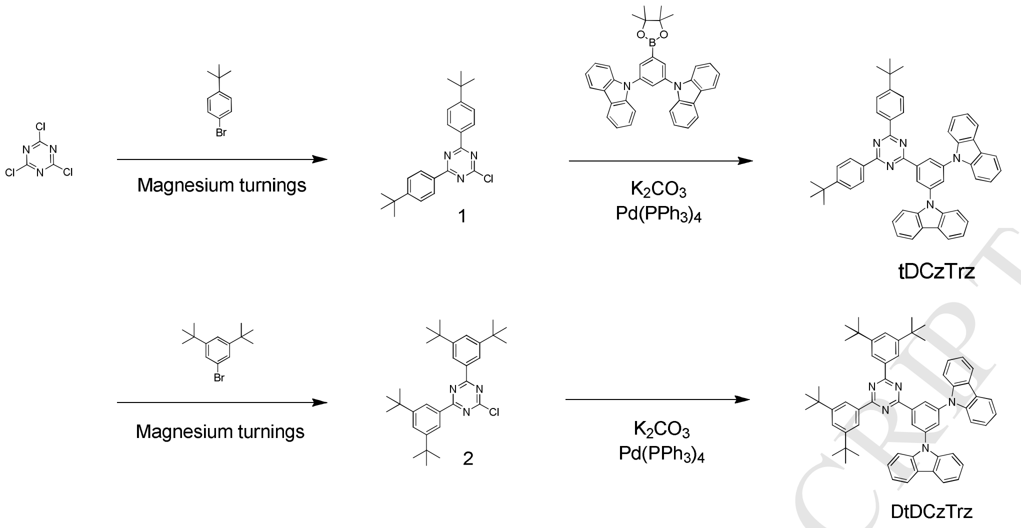

Scheme 1. Synthetic scheme of tDCzTrz and DtDCzTrz.

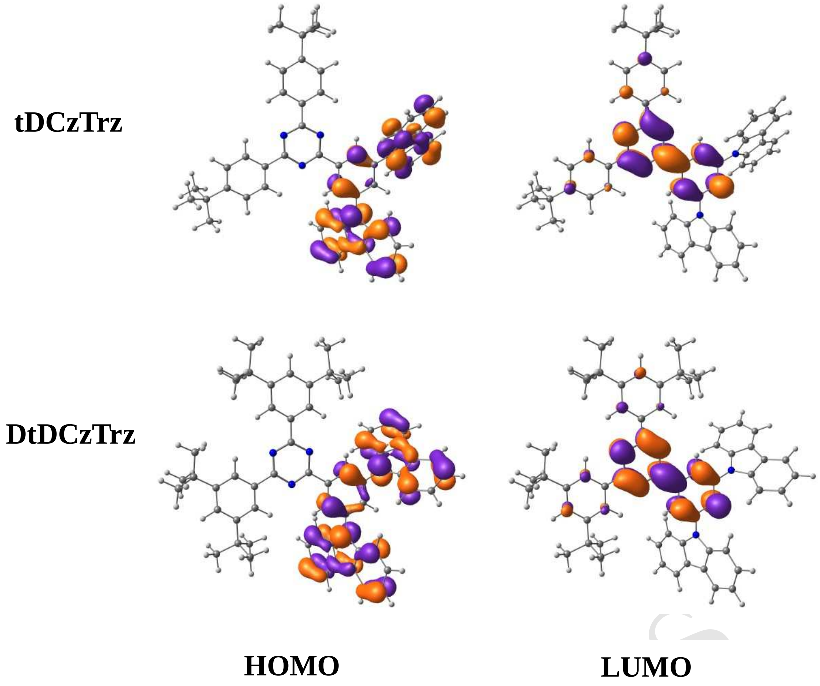

Figure 1. HOMO and LUMO distribution of tDCzTrz and DtDCzTrz calculated using Gaussian 09 program.

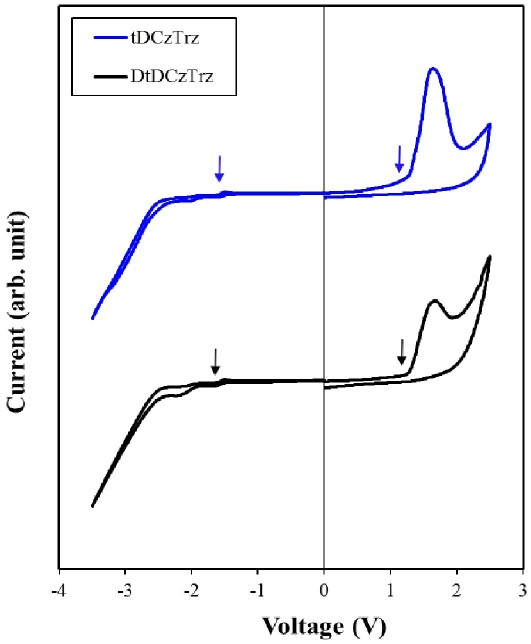

Figure 2. Electrochemical oxidation and reduction curves of tDCzTrz and DtDCzTrz.

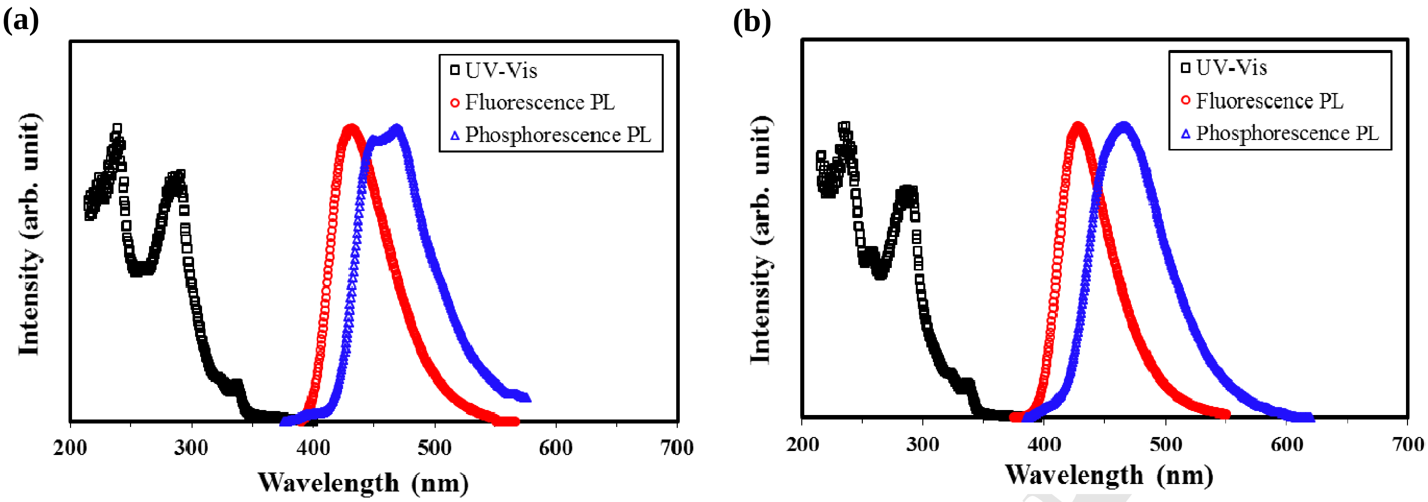

Figure 3. UV-Vis, fluorescence and phosphorescence spectra of the tDCzTrz (a) and DtDCzTrz (b). (Fluorescence spectra are prompt emission of solid film at room temperature and phosphorescence spectra are delayed emission spectra at 77 K.)

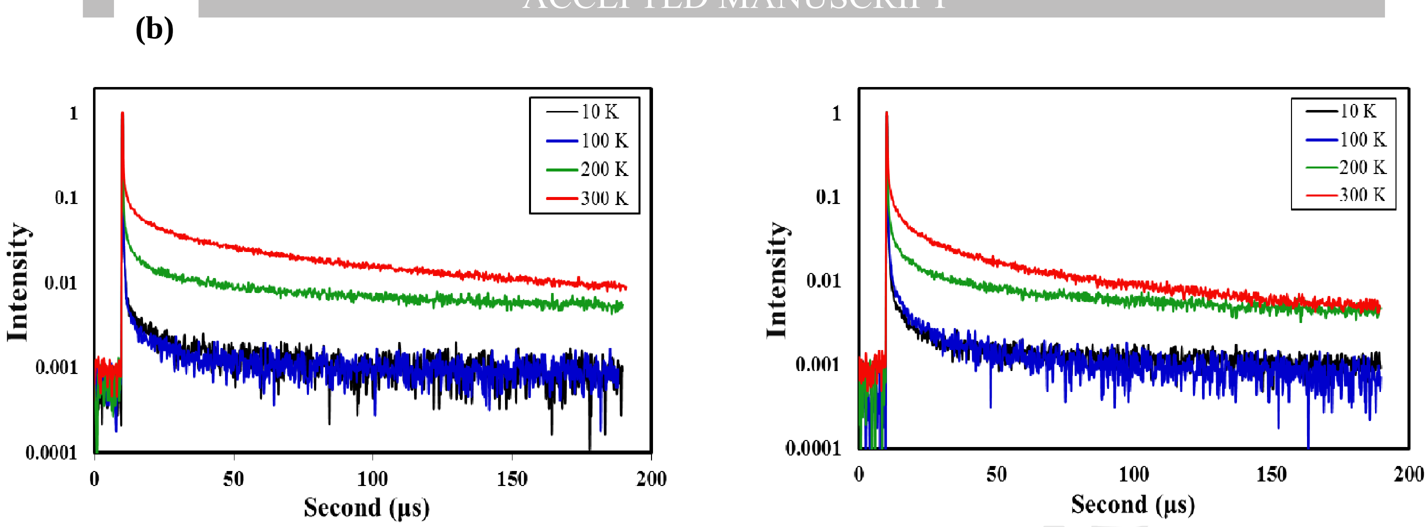

Figure 4. Transient PL decay curves of the 10 wt % tDCzTrz (a) and 20 w% DtDCzTrz (b) doped DPEPO films.

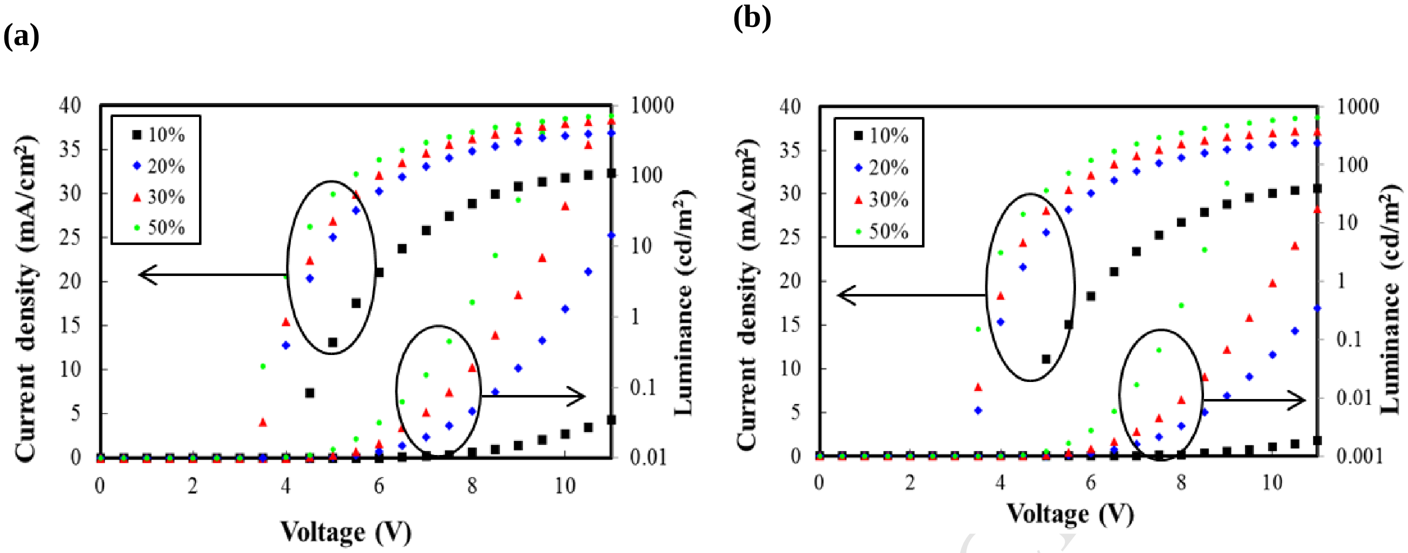

Figure 5. Current density-voltage-luminance curves of tDCzTrz (a) and DtDCzTrz (b) devices according to doping concentration of dopant materials.

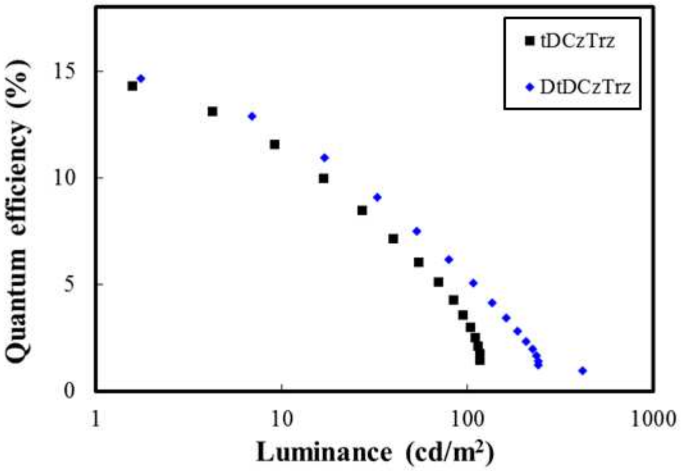

Figure 6. Quantum efficiency–luminance curves of tDCzTrz and DtDCzTrz devices at optimized doping concentration.

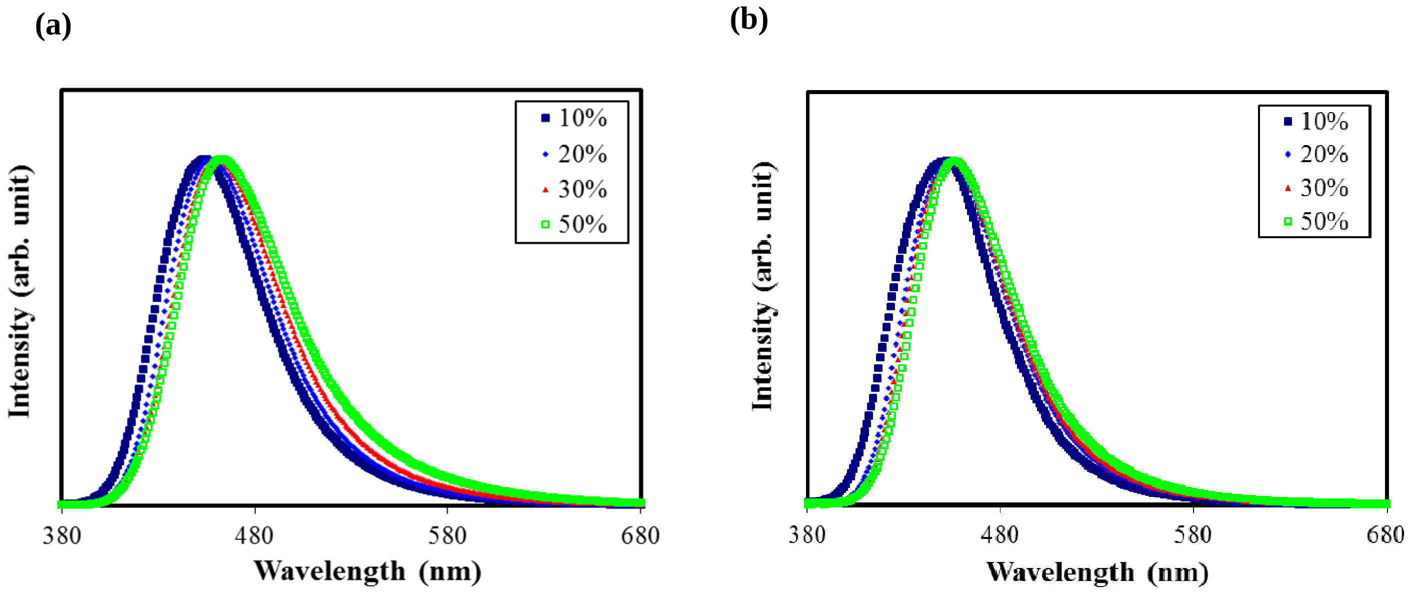

Figure 7. The electroluminescence (EL) spectra of tDCzTrz (a) and DtDCzTrz (b) devices according to doping concentration of dopant materials.

- A t-butyl modification of a triazine based acceptor moiety as an approach to manage the light-emitting properties of blue emitters
- Deep blue emission color in thermally activated delayed fluorescent organic light-emitting diodes by t-butyl substituent
- Stable emission spectrum according to the change of doping concentration